Metrological Characterization of Therapeutic Devices for Pressure Wave Therapy: Force, Energy Density, and Waveform Evaluation

Metrological characterization of therapeutic devices for pressure wave therapy: force, energy density and waveform evaluation

G. Cosoli, L. Verdenelli, and L. Scalise, *Member, IEEE*

***Abstract*— Pressure wave therapy is widespread for multiple purposes, from cell metabolism stimulation to tendons, ligaments, muscles and bones pathologies treatment. However, in the literature there are no quantitative metrological data related to pressure wave devices. On the contrary, it would be extremely important to have more information on the provided therapeutic signal, which could also be exploited as input for a finite element model able to foresee the pressure waves propagation inside the tissues. The authors investigated three different versions of the same device in terms of force applied to the tissue. The results show a high variability of the pulses intensities (up to 25 %), highlighting a non-uniformity of the treatment (in particular at low frequencies and high compressed air pressure). Moreover, the dependence from different parameters (i.e. pulse frequency, pressure, opening time of the solenoid valve for the compressed air pushing the bullet) was investigated. It was found that the lower the frequency and the higher the opening time of the valve, the higher the force applied to the tissue. An estimation of energy density was done; sometimes the limit values provided by pressure wave therapy guidelines (i.e. DIGEST and ISMST) are exceeded, in particular for soft tissues.**

***Index Terms*— pressure wave therapy, metrological characterization, force measurement, FEM simulation**

I. Introduction

Pressure wave therapy is increasingly widespread, thanks to its multiple benefits: metabolism stimulation, blood flow enhancement, tissue regeneration promotion, elimination of pathological alterations of tendons, ligaments, muscles and bones [1]–[7]. This kind of treatment consists in the supply of a burst of pulses on the tissue to be treated; these pulses are generated by means of an accelerated bullet (pushed with compressed air) hitting a solid body, whose motion is transferred to the tissue [8], [9]. An example of a typical handpiece of a pressure wave device is reported in Fig. 1.

The healthcare professional has to select different parameters to properly tune the therapy according to the patient necessities: how many pulses have to be supplied, their frequency and the pressure value for the bullet acceleration [10], [11].

In spite of the popular use of this technique, to the best of the authors' knowledge, very few quantitative data are reported in the literature about the metrological characteristics of the therapeutic device and the accuracy of the signal supplied to the tissues. There are only some guidelines, such as DIGEST and ISMST [10], [11], reporting approximate limits in terms of energy density provided to the treated tissues. However, it would be more interesting to know how much of the force acting on the tissue surface reaches a layer at a determined depth, as well as how the therapy varies with different parameters.

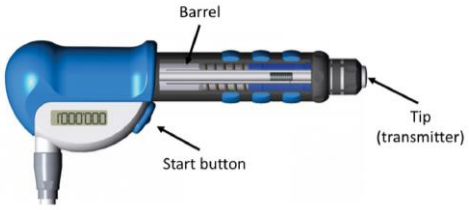

Fig. 1. Typical handpiece of a pressure wave device; the transmitter is put in contact with the tissue to be treated and the pulses supply is started by pushing the start button, activating the solenoid valve providing the compressed air to push the bullet along the barrel.

A Finite Element Model could be conceptualized to represent a tissue submitted to a determined force (that is the one provided through the therapeutic device), in order to evaluate how the pressure waves propagate inside the different tissue layers and which force values they are subjected to. Furthermore, a numeric model can help in better understanding the underlying mechanism for the therapy [12], [13]. In Fig. 2 an example of FEM result (from a model developed by the authors, with COMSOL Multiphysics software [14]) is reported, representing the waves propagation in a connective tissue layer when 18 MPa pressure is applied by the transmitter surface.

Such a kind of numerical models can be used as soft sensors, capable to estimate quantities difficultly measurable with standard sensors in real conditions [15] (for example, a soft sensor could be used to derive energy density starting from compressed air pressure), besides being an ideal instrument for the optimization of the device design [16].

In a previous study [17], the authors did a preliminary metrological characterization of a pressure wave therapeutic device considering the tip displacement and the provided force (which the energy density can be derived from). The signal considered consisted in 350 pulses at 1 Hz with different pressure values.

This paper aims at extending that study, considering more versions of a non-commercial pressure wave therapeutic device and more combinations of the parameters of interest (i.e. number of pulses, frequency, compressed air pressure, but also opening times of the solenoid valve controlling the air to push the bullet along the barrel).

TABLE I
PROPERTIES OF THE DEVICE UNDER TEST (DUT1, DUT2, AND DUT3)

Property	Value
Compressed air pressure	1.5 – 5 bar
Frequency	1 – 20 Hz
Nr. of pulses	Up to 10000
Modality	Single pulse/Burst of pulses Manual/Automatic
Solenoid valve opening times	10 – 20 ms

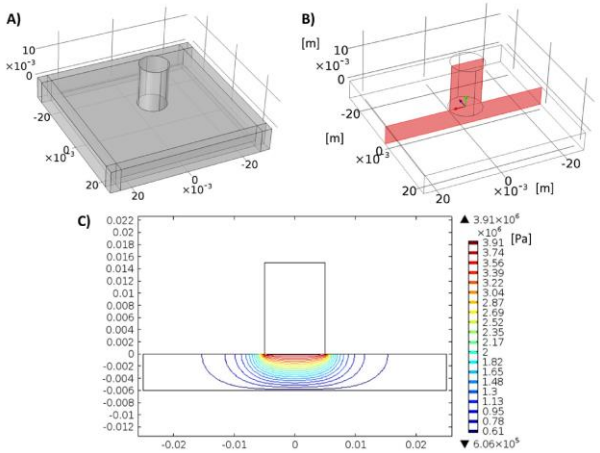

Fig. 2. Simplified model (realized with COMSOL Multiphysics software [14]) of a skin layer (parallelepiped shape) put in contact with the transmitter of the pressure wave device (cylindric shape) (A). The propagation of the pressure wave (C) is reported on a frontal section selected on the model (B); isolines of maximal pressure are reported.

II. Materials and Methods

Two measurement campaigns were carried out:

1. On one pressure wave device, DUT1 (DUT stands for Device Under Test);
2. On two pressure wave devices, DUT2 and DUT3, with different solenoid valve models (between the two, in terms of opening times) installed in the handpiece.

They are three different versions of a same device, which is not commercially available as a single device, but specifically realised by the producer of the pressure wave therapy device to perform this investigation. Their characteristics are reported in Table I.

A. Measurement campaign n°1

The first measurement campaign, carried out on DUT1, explored all the possible combinations of the following parameters:

- Opening times of the solenoid valve: 10, 15, 17 and 20 ms;
- Compressed air pressure: 1.5, 2, 3, 4 and 5 bar;
- Frequency of the pulses: 1, 5, 10, 15 and 20 Hz.

All the tests were carried out on 100 pulses and were repeated 3 times for each configuration, in order to evaluate the repeatability of the provided therapeutic signal.

B. Measurement campaign n°2

The second measurement campaign considered different parameters for the two considered devices (DUT2 and DUT3, in the following). In particular, for DUT2:

- Opening time of the solenoid valve: 10 ms;
- Compressed air pressure: 1.5, 3 and 5 bar;
- Frequency of the pulses: 1, 10 and 20 Hz.

Instead, for DUT3, the following parameters were considered:

- Opening time of the solenoid valve: 15, 17 and 20 ms;
- Compressed air pressure: 1.5, 3 and 5 bar;
- Frequency of the pulses: 1, 10 and 20 Hz.

For all the tests 100 pulses were supplied.

C. Data acquisition

The measurement setup is reported in Fig. 3.

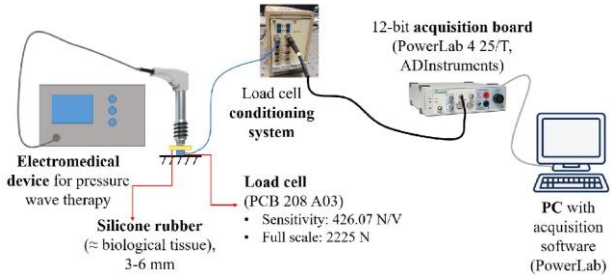

Fig. 3. Test bench for the measurement of the transmitted force by means of a load cell; the acquired signal was converted into digital through a 12-bit ADC board, connected to a PC provided with a proper acquisition software.

The force applied by the transmitter was measured by means of a piezoelectric load cell (PCB 208 A03, sensitivity of the calibrated sensor: 447.50 N/V; full scale: 2225 N, natural frequency: 70 kHz [18]), which was fastened to the test table by means of beeswax. The force transducer is suitable to measure the typical waveform generated by the device under test, as its rise time and duration are in the order of nanoseconds [17]. In order to simulate a biological tissue, a 3 mm rubber (whose acoustic properties reported in Table II) was inserted between the transmitter and the cell; therefore, the measured force is that in correspondence of a 3 mm depth. The load cell was connected to a 12-bit ADC board (PowerLab 4/25T, ADInstruments [19]), attached to a PC equipped with LabChart acquisition software (LabChart 7, ADInstruments [20]). The sampling frequency was equal to 10 kHz, since the main frequency content of the signal is < 3 kHz, as it is possible to note in the frequency spectrum reported in Fig. 4. Moreover, an anti-aliasing filters bank was included in the measurement setup.

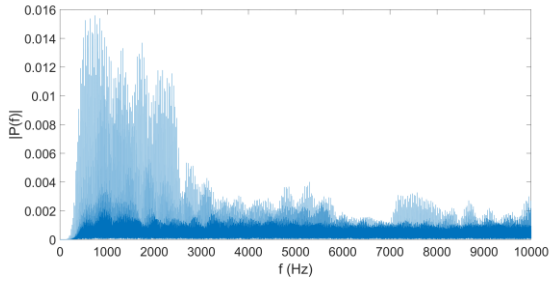

Fig. 4. Frequency spectrum of a typical pressure wave signal.

D. Data processing

With regard to data processing, the signal was first of all calibrated according to the sensitivity of the load cell (i.e. 447.5 N/V).

The following step consisted in identifying all the peaks of the pulses, according to the definition of a proper amplitude threshold and a minimum temporal distance between two consecutive peaks. Then, the average and the standard deviation of the amplitudes were computed; in this way, the distribution of the pulses intensity (and, therefore, the uniformity of the treatment) was evaluated. Also the average waveform of the total number of pulses for each configuration was computed.

The energy density (as defined in IEC 61846 Ultrasonics–Pressure pulse lithotripters–Characteristics of fields [21, P. 61846]) was computed according to the equation reported below [22], [23] and the results obtained for rubber were transferred to some biological tissues (i.e. skin, connective tissue and bone), in order to have approximate values to compare with the reference guidelines. The values of tissue density and sound velocity were taken from the literature [8], [24], [25] and are reported in Table II.

$$energy\ density = \frac{1}{A^2 \rho_0 c_0} \int F^2 dt \quad [\mathrm{J/m^2}]$$

where:

- A [m^2] is the transmitter area;
- ρ_0 [kg/m^3] is the tissue density;
- c_0 [m/s] is the sound velocity in the tissue; $\rho_0 c_0$ is the acoustic impedance of the tissue;
- F [N] is the measured force, with the simplifying assumption of uniform distribution on the sensing surface.

Finally, comparisons were done with regard to frequency and opening time of solenoid valve parameters.

TABLE II
DENSITY, YOUNG'S MODULUS AND SOUND VELOCITY OF THE DIFFERENT MATERIALS CONSIDERED

Material	Density (kg/m^3)	Young's modulus (MPa)	Sound velocity (m/s)
Rubber	1400	20	948
Skin	1109	15	1624
Connective tissue	1027	17	1545
Cortical bone	1908	>20000	3515

III. Results

In this section, results are reported in terms of force and energy density, for the two separate measurement campaigns.

A. *Results of the measurement campaign n°1*

An example of a force histogram and the corresponding average waveform are reported in Fig. 5 and Fig. 6, respectively, for compressed air pressure equal to 3 bar, opening time of the solenoid valve equal to 10 ms and 1 Hz frequency. These results were obtained on 300 pulses (i.e. the total number of pulses on 3 repeated tests).

For the sake of brevity, not all the results for all the possible configurations are reported, but only summary plots comparing force values with regard to specific parameters. In particular, in Fig. 7 there is a bar plot representing force mean values and standard deviations at different compressed air pressure values (from 1.5 to 5 bar) with respect to the time opening of the solenoid valve, considering a pulse frequency of 10 Hz. The measurement intervals (i.e. $\mu \pm \sigma$, where μ is the mean and σ the standard deviation) resulting from slightly varying compressed air pressure values (e.g. 1.5 and 2 bar, or 4 and 5 bar) are generally compatible, so the differences are not statistically significant.

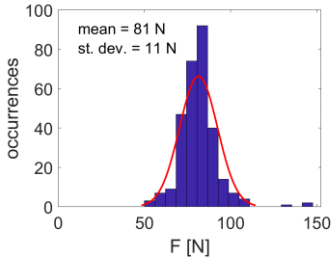

Fig. 5. Histogram of the applied force values for 300 pulses at 3 bar, 1 Hz frequency and opening time of the solenoid valve equal to 10 ms (DUT1).

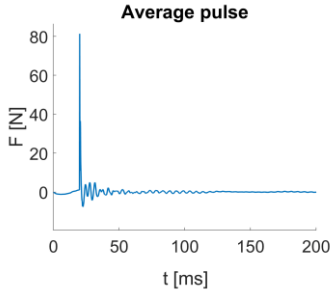

Fig. 6. Average pressure pulse waveform obtained on 300 pulses at 3 bar, 1 Hz frequency and opening time of the solenoid valve equal to 10 ms (DUT1).

It can be noticed that the higher the opening time of the solenoid valve, the higher the applied force, except for the highest opening time value (i.e. 20 ms), when the force applied to the tissue seems to start decreasing. The same considerations can be made for the other frequency values. On the contrary, when the opening time of the solenoid valve is not long enough, the bullet is not accelerated enough: this results in a "fake" impact into the transmitter, due only to the compressed air and not to the bullet.

In Fig. 8 there is a bar plot representing force mean values and standard deviations at different compressed air pressure values (from 1.5 to 5 bar) with respect to the pulse frequency values (from 1 to 20 Hz), considering a time opening for the solenoid valve equal to 20 ms. As already observed for Fig. 7, there is no statistically significant differences between the results obtained for slightly varying compressed air pressure values. Force decreases with frequency, probably becsuse of limitations linked to the pressure reservoir refilling.

It can be stated that, all the other parameters being equal, the higher the frequency of the pulses, the lower the force applied to the tissues. Moreover, at high frequencies (i.e. 15 and 20 Hz) the force applied at 4 or 5 bar is approximately the same (i.e. there are no statistically significant differences). With regard to the variability of the provided pulses, it can be noticed that there is a higher standard deviation of the intensity at higher pressure values (in particular at low frequencies); this could be due to the frequency of the pressure reservoir refilling, which should be greater when a higher pressure is required.

With regard to energy density results, an example is reported in Fig. 9 for 10 Hz frequency and an opening time of the solenoid valve equal to 20 ms.

The same kind of considerations can be made in terms of energy density. The corresponding plots are reported in Fig. 10 and Fig. 11, respectively, for simulated connective tissue.

It can be observed that the limit reported in the guidelines (i.e. 300 J/m^2) is never exceeded for the configurations reported and it is confirmed for all the tested configurations.

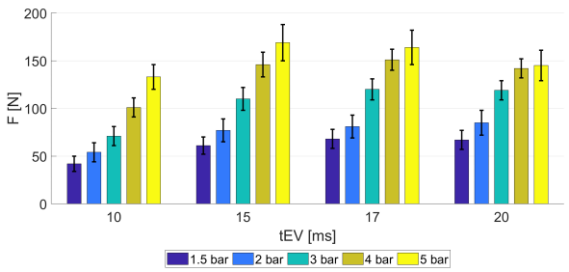

Fig. 7. Force values at different compressed air pressure values (i.e. 1.5, 2, 3, 4 and 5 bar) with respect to opening time of the solenoid valve (i.e. 10, 15, 17 and 20 ms) at 10 Hz frequency (DUT1).

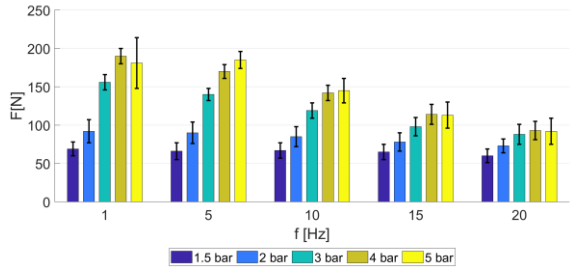

Fig. 8. Force values at different compressed air pressure values (i.e. 1.5, 2, 3, 4 and 5 bar) with respect to pulses frequency values (i.e. 1, 5, 10, 15 and 20 Hz) with an opening time of the solenoid valve equal to 20 ms (DUT1).

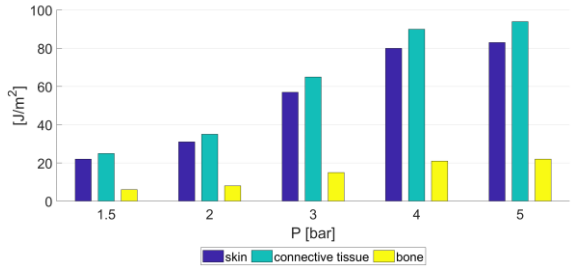

Fig. 9. Energy density values at different compressed air pressure values (i.e. 1.5, 2, 3, 4 and 5 bar) for different kinds of simulated tissue (i.e. skin, connective tissue and bone) at 10 Hz frequency and 20 ms opening time of the solenoid valve (DUT1).

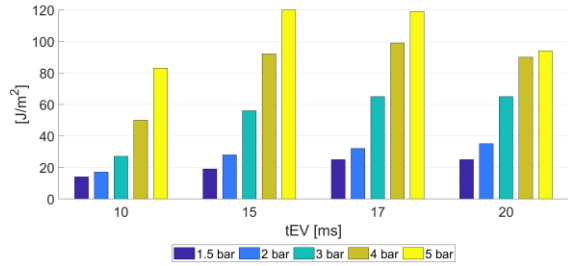

Fig. 10. Energy density values for simulated connective tissue at different pressures set for the compressed air (i.e. 1.5, 2, 3, 4 and 5 bar) with respect to opening time of the solenoid valve (i.e. 10, 15, 17 and 20 ms) at 10 Hz frequency (DUT1).

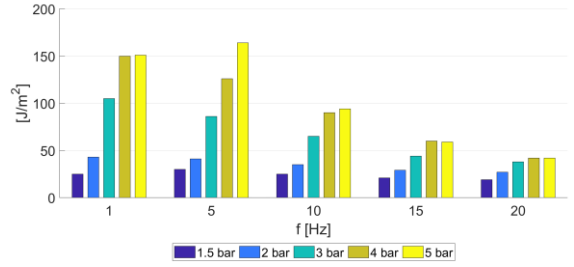

Fig. 11. Energy density values for simulated connective tissue at different compressed air pressure values (i.e. 1.5, 2, 3, 4 and 5 bar) with respect to pulses frequency values (i.e. 1, 5, 10, 15 and 20 Hz) with an opening time of the solenoid valve equal to 20 ms (DUT1).

B. Results of the measurement campaign n°2

With regard to the second measurement campaign, results are reported in the same manner as in the previous one: an example of the histogram of the force values and the corresponding average pressure waveform, an example of the energy density values for the different simulated tissues and then, for the sake of brevity, some comparative bar plots. Furthermore, results are reported for the two different handlers tested in this measurement campaign. It is worthy to notice that only three values of compressed air pressure have been tested, since, according to the results obtained from the previous measurement campaign, measurement intervals for slighlty different values are compatible.

In particular, in Fig. 12 and Fig. 13 the histogram and the average waveform are reported, respectively, for pressure equal to 3 bar and 10 Hz frequency for DUT2. These results were obtained on 100 pulses.

With regard to energy density results, an example is reported in Fig. 14 for 10 Hz frequency for DUT2.

In Fig. 15 and Fig. 16 there are bar plots representing, respectively, force mean values and standard deviations at different compressed air pressure values (i.e. 1.5, 3 and 5 bar) with respect to the pulse frequency values and the corresponding energy density values, both for the DUT2.

It can be noticed that the highest variability in the provided pulses is observed at high compressed air pressure value (i.e. 5 bar) and low frequency (i.e. 1 Hz), probably because of an incorrect setting for the pressure reservoir refilling. It is worth noting that, even if this is an indirect estimation of energy density, the guidelines limit value (i.e. 300 J/m^2) seems to be exceeded at high compressed air pressure, above all at lower frequencies (which represent critical conditions for the system, resulting also in higher variability).

The higher the pulses frequency, the lower the force (and, consequently, the energy density) applied to the treated tissue.

With regard to DUT3, an example of histogram of pulses intensities and the corresponding average waveform are reported in Fig. 17 and Fig. 18, respectively, for compressed air pressure equal to 3 bar, 10 Hz frequency and opening time of the solenoid valve equal to 17 ms. For what concerns energy density results, an example is reported in Fig. 19 for 10 Hz frequency and an opening time of the solenoid valve equal to 20 ms.

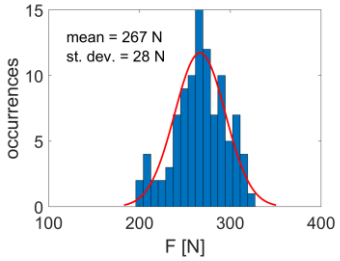

Fig. 12. Histogram of the applied force values for 100 pulses at 3 bar and 10 Hz frequency (DUT2).

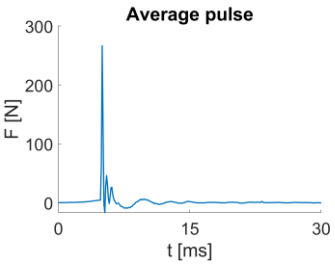

Fig. 13. Average pressure pulse waveform obtained on 100 pulses at 3 bar and 10 Hz frequency (DUT2).

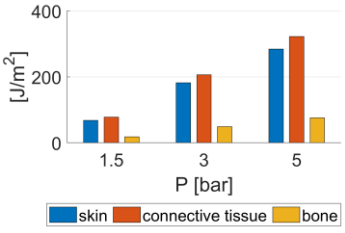

Fig. 14. Energy density values at different compressed air pressure values (i.e. 1.5, 3 and 5 bar) for different kinds of simulated tissue (i.e. skin, connective tissue and bone) at 10 Hz frequency (DUT2).

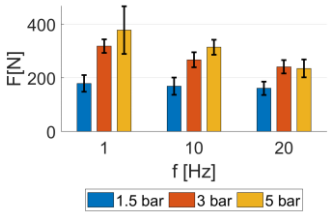

Fig. 15. Force values at different compressed air pressure values (i.e. 1.5, 3 and 5 bar) with respect to pulses frequency values (i.e. 1, 10 and 20 Hz) (DUT2).

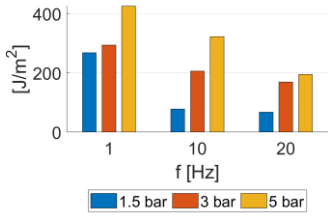

Fig. 16. Energy density values for simulated connective tissue at different compressed air pressure values (i.e. 1.5, 3 and 5 bar) with respect to pulses frequency values (i.e. 1, 10 and 20 Hz) (DUT2).

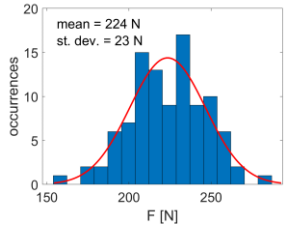

Fig. 17. Histogram of the applied force values for 100 pulses at 3 bar, 10 Hz frequency and opening time of the solenoid valve equal to 17 ms (DUT3).

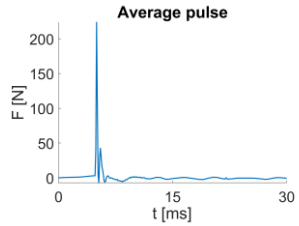

Fig. 18. Average pressure pulse waveform obtained on 100 pulses at 3 bar, 10 Hz frequency and opening time of the solenoid valve equal to 17 ms (DUT3).

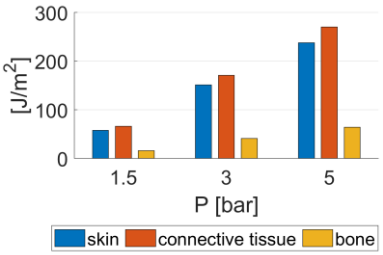

Fig. 19. Energy density values at different compressed air pressure values (i.e. 1.5, 3 and 5 bar) for different kinds of simulated tissue (i.e. skin, connective tissue and bone) at 10 Hz frequency and an opening time of the solenoid valve equal to 20 ms (DUT3).

In Fig. 20 and Fig. 21 there are bar plots representing, respectively, force mean values and standard deviations at different compressed air pressure values (i.e. 1.5, 3 and 5 bar) with respect to the pulse frequency values and the corresponding energy density values, both for the DUT3, for an opening time of the solenoid valve equal to 20 ms.

It can be noticed that the higher the pulses frequency, the lower the force applied to the tissue and, consequently, the lower the energy density provided. It is possible to notice that, in general (except for 5 bar, 20 Hz configuration), differences between two next compressed air pressure values are statistically significant (not compatible measurement intervals). Therefore, the treatment carried out with them is actually different (contrary to what observed for the values considered in the first measurement campaign).

In Fig. 22 and Fig. 23 there are bar plots representing, respectively, force mean values and standard deviations at different compressed air pressure values (i.e. 1.5, 3 and 5 bar) with respect to the opening time of the solenoid valve and the corresponding energy density values, both for the DUT3, for 10 Hz frequency.

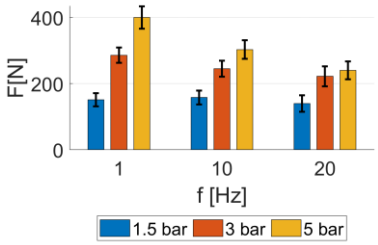

Fig. 20. Force values at different compressed air pressure values (i.e. 1.5, 3 and 5 bar) with respect to pulses frequency values (i.e. 1, 10 and 20 Hz) with an opening time of the solenoid valve equal to 20 ms (DUT3).

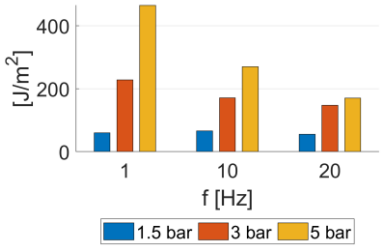

Fig. 21. Energy density values for simulated connective tissue at different compressed air pressure values (i.e. 1.5, 3 and 5 bar) with respect to pulses frequency values (i.e. 1, 10 and 20 Hz) with an opening time of the solenoid valve equal to 20 ms (DUT3).

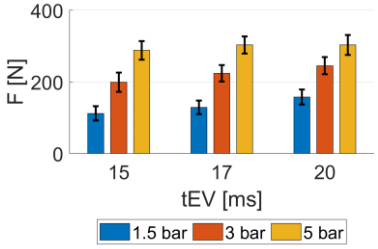

Fig. 22. Force values at different compressed air pressure values (i.e. 1.5, 3 and 5 bar) with respect to opening time of the solenoid valve (i.e. 15, 17 and 20 ms) at 10 Hz frequency (DUT3).

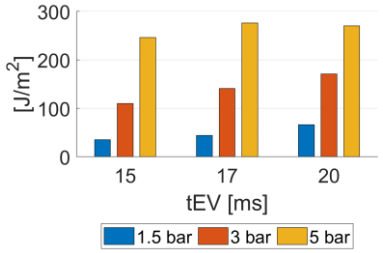

Fig. 23. Energy density values for simulated connective tissue at different compressed air pressure values (i.e. 1.5, 3 and 5 bar) with respect to opening time of the solenoid valve (i.e. 15, 17 and 20 ms) at 10 Hz frequency (DUT3).

In this case, the higher the opening time of the solenoid valve, the higher the force (and, consequently, the energy density) provided, since the bullet is subjected to compressed air for a greater time interval.

IV. Conclusions

The application of pressure wave therapy is increasingly widespread, however the quantitative parameters influencing the therapeutic outcome have not been deeply explored so far.

In this study the authors evaluated three different versions of the same device; from the results, it can be stated that:

- the higher the opening time of the solenoid valve, the higher the applied force (and, consequently, the energy density);
- the opening time of the solenoid valve should be sufficient to avoid "fake shots"; 15, 17 and 20 ms were proved to be suitable, whereas 10 ms is too short;
- the higher the frequency of the pulses, the lower the force (and, consequently, the energy density) applied to the treated tissues; this could be linked to a not sufficiently high ferquency of the pressure reservoir filling, which should be improved in future versions of the device;
- variability of pulses is greater (up to 25%) at higher compressed air pressure and low frequencies, representing critical conditions for the system; in standard therapeutic conditions, variability is <10%;
- measurement intervals (i.e. $\mu \pm \sigma$) obtained with slightly different compressed air pressure values (e.g. 4 and 5 bar) are compatible. Consequently, it is worthy to reduce the selectable values for the pressure driving the therapy.

Particular attention has to be paid when deriving energy density from the measured force, because literature values are used for density and sound velocity values, but variability of physiological quantities is high. It is worthy to underline the fact that the signals generated by the device under test are slower than those reported in ISMST guidelines, since the waveform has both rise time and duration in the order of nanoseconds. However, slower values (in the order of milliseconds) are reported in literature, where it is said that the waveform is distorted by the means of the impact body [26]. For this reasons, results cannot be compared to those reported in literature for faster signals, as in [27], both in terms of duration and intensity.

The measured force data could be used in a finite element model to visualize the pressure waves propagation inside a determined tissue (or through layers of different tissues, showing different acoustic properties [28]). This would allow the therapist to tune parameters according to the desired effect at a determined depth in the tissue, where, for example, a pathology has been located by means of standard diagnostic methods (e.g. x-ray or ultrasound technique). Indeed, therapists usually choose pulses number, frequency and pressure value according to DIGEST and ISMST guidelines or based on their experience, but it would be of utmost importance to have an objective tool able to predict the effects of the therapy on the treated tissues not only qualitatively. This could be a numeric model, having as inputs mechanical quantities measured on the therapeutic device. Such an instrument could foresee what would happen if a determined parameter was changed, also providing a kind of soft sensor, able to estimate the intensity of the pressure wave supplied to the tissues to be treated. Indeed, as already highlighted in literature for several medical devices, the future trend is focused on soft sensors, which allow the therapist to know in real-time useful parameters (e.g. energy density, in case of pressure wave therapy) estimated from previously measured/simulated data (e.g. compressed air pressure). Soft sensors are used not only in biomedical applications [29]–[31], but also in different fields, such as industrial [32], [33], smartphone [34] and building [35] applications. For example, starting from the parameters set in the pressure wave device (e.g. compressed air pressure and frequency), a soft sensor could estimate the energy density provided to the treated tissue, which is a quantity not easily measurable in real applications. Besides, numerical models are often used in biomedical applications, in order to better understand occurring phenoemena and, consequently, to optimize the design of therapeutic devices [36]–[40].

Measurements and models of this kind are also useful to improve the electromedical device design in order to have a more uniform treatment on the tissues, since high variability can be observed in the results (up to 25% in terms of pulses intensity). Also indications for the controlling software of the device can be obtained, for example concerning the pressure reservoir refilling.

Finally, it is possible to make an approximative evaluation of energy density parameter, to be compared to guidelines values. Even if these are not compulsory limits to respect, it is worth thinking, in medical terms, what a higher energy value could entail for the patient. Within 2020 a standard specific for non-focusing pressure pulse sources (i.e. IEC 63045 Ultrasonics - Non-focusing pressure pulse sources - Characteristics of fields, currently under development by the IEC technical committee TC87 [41], [42, p. 87]) should be published; this will be of utmost importance to measure field parameters in a reliable and repeatable way.

It would be interesting to realize an instrumented prototype able to collect real data during a real treatment, so as to study what happens in tissues during the procedure. This would overcome the limits of the present results in terms of energy density, since measurements were carried out on a tissue phantom and the results were transferred to tissues by means of literature data in terms of density and sound velocity, which are characterized by a high variability.

REFERENCES

[1] C.-J. Wang *et al.*, 'Shock wave therapy induces neovascularization at the tendon-bone junction. A study in rabbits', *J. Orthop. Res. Off. Publ. Orthop. Res. Soc.*, vol. 21, no. 6, pp. 984–989, Nov. 2003, doi: 10.1016/S0736-0266(03)00104-9.

[2] W. Schaden *et al.*, 'Shock wave therapy for acute and chronic soft tissue wounds: a feasibility study', *J. Surg. Res.*, vol. 143, no. 1, pp. 1–12, Nov. 2007, doi: 10.1016/j.jss.2007.01.009.

[3] A. Saxena, L. St., and M. Fournier, 'Vibration and pressure wave therapy for calf strains: A proposed treatment', *Muscles Ligaments Tendons J.*, vol. 3, no. 2, pp. 60–62, 2013, doi: 10.11138/mltj/2013.3.2.060.

[4] S. R. McClure, I. M. Sonea, R. B. Evans, and M. J. Yaeger, 'Evaluation of analgesia resulting from extracorporeal shock wave therapy and radial pressure wave therapy in the limbs of horses and sheep', *Am. J. Vet. Res.*, vol. 66, no. 10, pp. 1702–1708, 2005, doi: 10.2460/ajvr.2005.66.1702.

[5] F. E. T. Pauwels, S. R. McClure, V. Amin, S. Van, and R. B. Evans, 'Effects of extracorporeal shock wave therapy and radial pressure wave therapy on elasticity and microstructure of equine cortical bone', *Am. J. Vet. Res.*, vol. 65, no. 2, pp. 207–212, 2004, doi: 10.2460/ajvr.2004.65.207.

[6] I. Wijayanti, I. N. Murdana, T. Z. Tamin, and A. Kekalih, 'Comparing the effectiveness of medium- and high-dose extracorporeal shockwave therapy against calcific tendonitis of the rotator cuff', *J. Phys. Conf. Ser.*, vol. 1073, p. 042025, Aug. 2018, doi: 10.1088/1742-6596/1073/4/042025.

[7] A. García-Muntión, L. Godefroy, H. Robert, D. Muñoz-García, C. Calvo-Lobo, and I. López-de-Uralde-Villanueva, 'Study of the mechanisms of action of the hypoalgesic effect of pressure under shock waves application: A randomised controlled trial', *Complement. Ther. Med.*, vol. 42, pp. 332–339, 2019, doi: 10.1016/j.ctim.2018.12.012.

[8] P. Tsaklis, 'Presentation of Acoustic Waves Propagation and Their Effects Through Human Body Tissues', *Hum. Mov.*, vol. 11, no. 1, pp. 58–65, 2010, doi: 10.2478/v10038-009-0025-z.

[9] F. Ueberle and A. J. Rad, 'Ballistic pain therapy devices: measurement of pressure pulse parameters', *Biomed. Eng. Tech.*, vol. 57, no. SI-1 Track-H, pp. 700–703, 2012.

[10] 'Home :: Digest e.V.' https://www.digest-ev.de/ (accessed Jan. 08, 2020).

[11] 'ISMST (The International Society for Medical Shockwave Treatment)', Jun. 13, 2017. https://www.shockwavetherapy.org/fileadmin/user_upload/ISMST_Guidelines.pdf (accessed Jan. 08, 2020).

[12] Z. K. Alkhamaali, A. D. Crocombe, M. C. Solan, and S. Cirovic, 'Finite element modelling of radial shock wave therapy for chronic plantar fasciitis', *Comput. Methods Biomech. Biomed. Engin.*, vol. 19, no. 10, pp. 1069–1078, Jul. 2016, doi: 10.1080/10255842.2015.1096348.

[13] M. Benoit, J. H. Giovanola, K. Agbeviade, and M. Donnet, 'Experimental Characterization of Pressure Wave Generation and Propagation in Biological Tissues', in *13th International Conference on Biomedical Engineering*, 2009, pp. 1623–1626.

[14] 'COMSOL Multiphysics®'. https://www.comsol.it/.

[15] W. Pan, Y. Shen, T. Liu, R. Yu, and P. Fu, 'Stress Estimation in Different Bone Layers Subject to Therapeutic Ultrasound in an Intelligent Bone System', *IEEE Trans. Instrum. Meas.*, vol. 64, no. 5, pp. 1204–1214, 2014.

[16] M. Passard, C. Barthod, M. Fortin, C. Galez, and J. Bouillot, 'Design and optimization of a low-frequency electric field sensor using Pockels effect', *IEEE Trans. Instrum. Meas.*, vol. 50, no. 5, pp. 1053–1058, 2001.

[17] G. Cosoli and L. Scalise, 'Metrological characterization of a therapeutic device for pressure wave therapy', *J. Phys. Conf. Ser.*, vol. 1110, p. 012001, Nov. 2018, doi: 10.1088/1742-6596/1110/1/012001.

[18] 'PCB Piezotronics, Inc.: Sensors to measure vibration, acoustics, force, pressure, load, strain, shock & torque'. http://www.pcb.com/ (accessed Jan. 08, 2020).

[19] 'PowerLab', *ADInstruments*. https://www.adinstruments.com/products/powerlab (accessed Jan. 08, 2020).

[20] 'LabChart', *ADInstruments*. https://www.adinstruments.com/products/labchart (accessed Jan. 08, 2020).

[21] 'IEC 61846 Ultrasonics–Pressure pulse lithotripters–Characteristics of fields', 1998.

[22] R. O. Cleveland and J. A. McAteer, 'Physics of Shock-Wave Lithotripsy', in *Smith's Textbook of Endourology*, A. D. S. MD, G. H. B. MD, G. M. P. MD, and L. R. K. MD, Eds. Wiley-Blackwell, 2012, pp. 527–558.

[23] A. M. Loske, 'The role of energy density and acoustic cavitation in shock wave lithotripsy', *Ultrasonics*, vol. 50, no. 2, pp. 300–305, 2010, doi: https://doi.org/10.1016/j.ultras.2009.09.012.

[24] H. Azhari, 'Appendix A: Typical Acoustic Properties of Tissues', in *Basics of Biomedical Ultrasound for Engineers*, John Wiley & Sons, Inc., 2010, pp. 313–314.

[25] P. A. Hasgall *et al.*, 'IT'IS Database for thermal and electromagnetic parameters of biological tissues'. IT'IS Foundation, 2015, [Online]. Available: http://www.itis.ethz.ch/db3-0.

[26] Wess, O., 'Physics and technology of shock wave and pressure wave therapy', in *News Letter ISMST (Vol. 1)*, 2006.

[27] R. O. Cleveland, P. V. Chitnis, and S. R. McClure, 'Acoustic Field of a Ballistic Shock Wave Therapy Device', *Ultrasound Med. Biol.*, vol. 33, no. 8, pp. 1327–1335, 2007, doi: https://doi.org/10.1016/j.ultrasmedbio.2007.02.014.

[28] R. Beigelbeck, H. Antlinger, S. Cerimovic, S. Clara, F. Keplinger, and B. Jakoby, 'Resonant pressure wave setup for simultaneous sensing of longitudinal viscosity and sound velocity of liquids', *Meas. Sci. Technol.*, vol. 24, no. 12, p. 125101, Oct. 2013, doi: 10.1088/0957-0233/24/12/125101.

[29] N. Raveendranathan *et al.*, 'From Modeling to Implementation of Virtual Sensors in Body Sensor Networks', *IEEE Sens. J.*, vol. 12, no. 3, pp. 583–593, Mar. 2012, doi: 10.1109/JSEN.2011.2121059.

[30] K. de O. A. de Moura and A. Balbinot, 'Virtual Sensor of Surface Electromyography in a New Extensive Fault-Tolerant Classification System', *Sensors*, vol. 18, no. 5, May 2018, doi: 10.3390/s18051388.

[31] K. Liu, Y. Inoue, and K. Shibata, 'Physical sensor difference-based method and virtual sensor difference-based method for visual and quantitative estimation of lower limb 3D gait posture using accelerometers and magnetometers', *Comput. Methods Biomech. Biomed. Engin.*, vol. 15, no. 2, pp. 203–210, 2012, doi: 10.1080/10255842.2010.522184.

[32] G. Cosoli, P. Chiariotti, M. Martarelli, S. Foglia, M. Parrini, and E. P. Tomasini, 'Development of a soft sensor for indirect temperature measurement in a coffee machine', *IEEE Trans. Instrum. Meas.*, vol. 69, no. 5, pp. 2164–2171, 2020, doi: 10.1109/TIM.2019.2922750.

[33] X. Yuan, Z. Ge, Z. Song, Y. Wang, C. Yang, and H. Zhang, 'Soft Sensor Modeling of Nonlinear Industrial Processes Based on Weighted Probabilistic Projection Regression', *IEEE Trans. Instrum. Meas.*, vol. 66, no. 4, pp. 837–845, Apr. 2017, doi: 10.1109/TIM.2017.2658158.

[34] C. Crema, A. Depari, A. Flammini, E. Sisinni, A. Vezzoli, and P. Bellagente, 'Virtual Respiratory Rate Sensors: An Example of A Smartphone-Based Integrated and Multiparametric mHealth Gateway', *IEEE Trans. Instrum. Meas.*, vol. 66, no. 9, pp. 2456–2463, Sep. 2017, doi: 10.1109/TIM.2017.2707838.

[35] F. Heidtmann and D. Soffker, 'Virtual Sensors for Diagnosis and Prognosis Purposes in the Context of Elastic Mechanical Structures', *IEEE Sens. J.*, vol. 9, no. 11, pp. 1577–1588, Nov. 2009, doi: 10.1109/JSEN.2009.2028767.

[36] G. Tognola *et al.*, 'Numerical modeling and experimental measurements of the electric potential generated by cochlear implants in physiological tissues', *IEEE Trans. Instrum. Meas.*, vol. 56, no. 1, pp. 187–193, 2007, doi: 10.1109/TIM.2006.887334.

[37] B. J. Jarosz, 'Interstitial instrumentation for therapeutic ultrasonic heating: modeling the discrete blood vessels', *IEEE Trans. Instrum. Meas.*, vol. 49, no. 2, pp. 260–264, 2000, doi: 10.1109/IMTC.1999.776815.

[38] W. Hou, P. X. Liu, M. Zheng, and S. Liu, 'A New Deformation Model of Brain Tissues for Neurosurgical Simulation', *IEEE Trans. Instrum. Meas.*, 2019, doi: 10.1109/TIM.2019.2909247.
[39] X. P. Liu, S. Xu, H. Zhang, and L. Hu, 'A new hybrid soft tissue model for visio-haptic simulation', *IEEE Trans. Instrum. Meas.*, vol. 60, no. 11, pp. 3570–3581, 2011, doi: 10.1109/TIM.2011.2161142.
[40] S. Stoecklin, A. Yousaf, T. Volk, and L. Reindl, 'Efficient wireless powering of biomedical sensor systems for multichannel brain implants', *IEEE Trans. Instrum. Meas.*, vol. 65, no. 4, pp. 754–764, 2015, doi: 10.1109/TIM.2015.2482278.
[41] F. Ueberle, 'Measurement Parameters for the characterization of unfocused Extracorporeal Pressure Pulse Sources-Standardization of Biomedical Equipment', presented at the 23rd International Congress on Acoustics, Aachen, Germany, Sep. 2019, Accessed: Jan. 07, 2020. [Online]. Available: https://pdfs.semanticscholar.org/bac3/7f4df03f795427bf9184b75f19ef2e36127b.pdf.
[42] 'IEC - TC 87 Dashboard > Projects: Work programme, Publications, Maintenance cycle, Project files, TC/SC in figures'. https://www.iec.ch/dyn/www/f?p=103:38:7923923343173::::FSP_ORG_ID,FSP_APEX_PAGE,FSP_PROJECT_ID:1281,23,23065 (accessed Jan. 07, 2020).

G. Cosoli was born in Chiaravalle, Ancona, AN, Italy in 1989. She received the B.S. degree in biomedical engineering and M.S. degree in electronic engineering from the Università Politecnica delle Marche (UNIVPM), Ancona, in 2011 and 2013, respectively. She received the Ph.D. degree in mechanical engineering from the same university in 2017.

From 2016 to date, she has been a Postdoctoral Research Fellow with the Department of Industrial Engineering and Mathematical Sciences (DIISM) of UNIVPM. She is the author of 7 articles and 22 conference proceedings. Her research interests include non-invasive physiological measurements, numerical modelling, mechanical measurements, signal processing and NDT.

Eng. Cosoli was a recipient of IEEE MeMeA 2015 Best Poster award.

L. Verdenelli was born in Jesi (AN), Italy in 1990. He received the B.S. and M.S. degree in Biomedical Engineering
from the Polytechnic University of Marche (UNIVPM), Ancona, Italy, in 2015 and 2018, respectively. He is currently achieving the Ph.D at the DIISM (Department of Industrial Engineering and
Mathematical Sciences) of the same university, since November 2018. His work is focused on the use of 3D printing techniques for the developments of innovative methodologies and systems in the medical field.

L. Scalise was born in Siena, SI, Italy in 1971. He received the M.S. degree in electronic engineering from the Università degli Studi di Ancona, Ancona, in 1996. He received the Ph.D. degree in mechanical measurement from the same Università degli Studi di Padova, Padova, in 1999. In 1999, he was a visiting researcher at the Twente University of Twente (The Netherland). From 2000 to 2015, he has been Research Assistant with the Department of Industrial engineering and Mathematical Sciences, at the Polytechnic University of Marche, Ancona (Italy). Since 2015, he is Associate Professor (in the same department) of Mechanical Measurement and Biomedical Instrumentation, Applied Measurement Techniques, Electronical System in Radiology and Electrical Measurement, at the Faculties of engineering and Medicine. He is the author of more than 50 papers, 130 conference proceedings, 13 chapters in international books and 4 international patents. His research focuses on measurement techniques (mechanical and electronical), particularly sensing systems, biomedical instrumentation, assistive technologies, e-health, and characterization of systems and materials.
He is member of IEEE (Instrumentation and Measurement Society), of the International Society for Optics and Photonics (SPIE), of the International Academy of Laser medicine and Surgery (IALMS) and of the Society of Experimental Mechanics (SEM).